Sulfur and lead isotopic evidence of relic Archean sediments in the Pitcairn mantle plume

Hélène Delavault[a,1,2], Catherine Chauvel[a], Emilie Thomassot[b], Colin W. Devey[c], and Baptiste Dazas[a]

[a]ISTerre, Université Grenoble Alpes, CNRS, 38000 Grenoble, France; [b]Centre de Recherches Pétrographiques et Géochimiques, Université de Lorraine and CNRS, 54501 Vandœuvre-Les-Nancy, France; and [c]Geomar Helmholtz Centre for Ocean Research Kiel, 24148 Kiel, Germany

The isotopic diversity of oceanic island basalts (OIB) is usually attributed to the influence, in their sources, of ancient material recycled into the mantle, although the nature, age, and quantities of this material remain controversial. The unradiogenic Pb isotope signature of the enriched mantle I (EM I) source of basalts from, for example, Pitcairn or Walvis Ridge has been variously attributed to recycled pelagic sediments, lower continental crust, or recycled subcontinental lithosphere. Our study helps resolve this debate by showing that Pitcairn lavas contain sulfides whose sulfur isotopic compositions are affected by mass-independent fractionation (S-MIF down to $\Delta^{33}S = -0.8$), something which is thought to have occurred on Earth only before 2.45 Ga, constraining the youngest possible age of the EM I source component. With this independent age constraint and a Monte Carlo refinement modeling of lead isotopes, we place the likely Pitcairn source age at 2.5 Ga to 2.6 Ga. The Pb, Sr, Nd, and Hf mixing arrays show that the Archean EM I material was poor in trace elements, resembling Archean sediment. After subduction, this Archean sediment apparently remained stored in the deep Earth for billions of years before returning to the surface as Pitcairn's characteristic EM I signature. The presence of negative S-MIF in the deep mantle may also help resolve the problem of an apparent deficit of negative $\Delta^{33}S$ anomalies so far found in surface reservoirs.

mantle plume | sulfur isotopes | geochemical modeling | EM I | Pitcairn

Oceanic island basalts (OIB) are isotopically diverse (1) and, in radiogenic (Sr, Nd, Pb, Hf) isotopic spaces, define trends to extreme mantle compositions ("endmembers") such as HIMU (high μ, with μ = $^{238}U/^{204}Pb$) and the two enriched mantles EM I and II (EM I with low $^{206}Pb/^{204}Pb$ and EM II with high $^{87}Sr/^{86}Sr$). These endmembers are all thought to have been generated by subduction of material into the asthenosphere over time (2), so determining the age and geological nature of their precursors is important to understand the geochemical evolution of the Earth. Although there appears to be consensus on the presence of recycled ancient oceanic crust in the source of HIMU (3, 4) and ancient clastic continental sediments in the source of EM II (5), the origin of the EM I signature is more controversial.

The Polynesian islands chains show examples of all these types of source signatures (3, 6–9). For example, Mangaia and Tubuai Islands in the Cook-Austral chain have the elevated $^{206}Pb/^{204}Pb$ ratios typical of HIMU compositions, islands from both the Society and Marquesas chains have the high $^{87}Sr/^{86}Sr$ that define EM II compositions, and Pitcairn lavas in the Pitcairn-Gambier chain have the very low $^{206}Pb/^{204}Pb$ at high $^{208}Pb/^{204}Pb$ that characterize EM I isotopic signatures.

Here we focus on EM I of Pitcairn Island [0.95 My to 0.62 My (10)] and the Pitcairn Seamounts (11), which constitute the most recent volcanism of the Pitcairn-Gambier chain, located on the southeast side of the Polynesian Superplume (Fig. 1). Previous studies of both the island and the seamounts led to various interpretations for the origin of the EM I source: recycled oceanic crust carrying 0.7- to 2-Ga pelagic sediment (12, 13), delaminated subcontinental lithospheric mantle (14), and delaminated lower continental crust (15). Each of these suggestions was an attempt to explain the peculiar Pb isotopic compositions of

Pitcairn basalts, but all remain model-dependent, as the problem is underdetermined. Independent constraints on either the age or the nature of the source component are therefore required to choose the best candidate.

Here we revisit the possible origin of the EM I signature by presenting in situ sulfur isotopic analyses of Pitcairn samples that provide independent constraints on a minimum age. Combining these data with modeling of new high-precision Pb isotopic data and Sr, Nd, and Hf isotopes allows us to constrain the nature of the material involved in their source.

Results and Discussion

The sulfur isotopic data measured on sulfide inclusions in olivines, plagioclases, and matrix material at Centre de Recherche Pétrographiques et Géochimiques (CRPG) in Nancy are given in *SI Appendix,* Table S1 and shown in Fig. 2. Pictures of the different sulfides are also reported in *SI Appendix,* Fig. S1. We note two important features of the measurements: (*i*) With one exception, all Pitcairn sulfides are characterized by both negative $\delta^{34}S$ (down to −6.2‰) and negative $\Delta^{33}S$ (down to −0.8‰) and so show evidence of mass-independent fractionation (hereafter "S-MIF"). Data on standards measured as unknowns together with the sample suite show the external reproducibility of the method to be ∼0.34‰ (2σ) on $\Delta^{33}S$ (see *SI Appendix* on sulfide analyses). The average $\Delta^{33}S$ value for post-Archean standards is within error of 0. Both these features demonstrate that the negative S-MIF measured in the Pitcairn samples is real and significant. (*ii*) Repeat measurements on one sulfide inclusion from the matrix (51DS-13) show a range of $\Delta^{33}S$ from −0.54 to 0.12 (*SI Appendix,* Table S1). Although this total range is larger than the external reproducibility, we note that (*i*) the average of these values is negative and (*ii*) the most positive values are within error of $\Delta^{33}S = 0$. Both these features suggest that the negative magmatic $\Delta^{33}S$ of this inclusion has been mixed with

Significance

The source material for mantle plume volcanism is generally agreed to show geochemical signatures of former oceanic lithosphere (crust and/or sediments) recycled into the mantle by subduction. The specific nature and ages of these materials remains, however, controversial. This study shows that the source of Pitcairn basalts contains Archean sediments (i.e. >2.45 Ga) that have remained chemically isolated in Earth's mantle for billions of years.

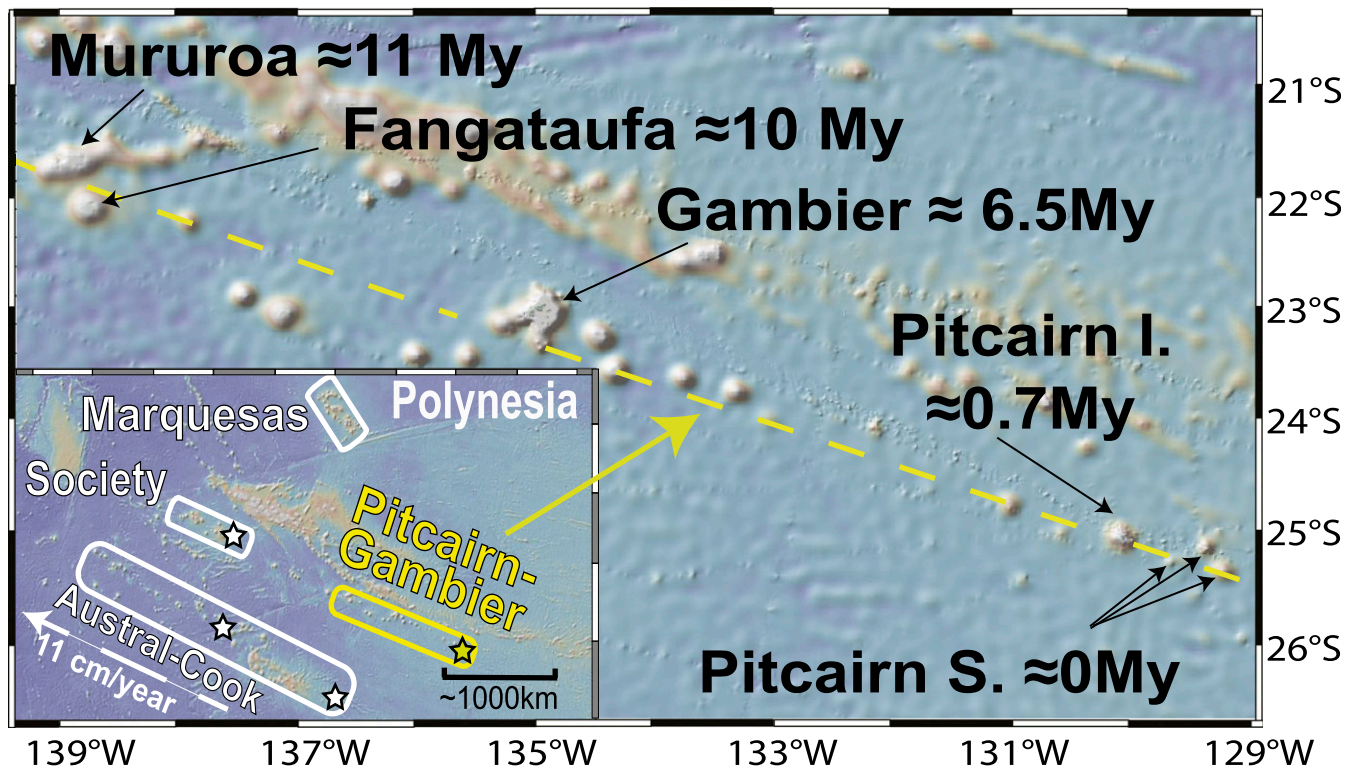EARTH, ATMOSPHERIC, AND PLANETARY SCIENCES

Fig. 1. Map of the Pitcairn-Gambier chain that includes Mururoa and Fangataufa atolls, the Gambier archipelago, Pitcairn Island (Pitcairn I.), and Pitcairn Seamounts (Pitcairn S.) with their associated ages. (*Inset*) The four chains that constitute Polynesia, as well as the locations of active volcanism (stars).

young, $\Delta^{33}S = 0$ material, probably from seawater; this may be the result of syneruptive or posteruptive seawater infiltration into the basaltic matrix. None of the inclusions in minerals show $\Delta^{33}S > 0$, which we suspect is a result of the better resistance of mineral structures to such syneruptive or posteruptive seawater infiltration.

Negative $\Delta^{33}S$ values have been previously reported for pyrite included in Archean barite bedded formations (16, 17), Neo-Archean carbonates (18, 19), exhalites in Archean greenstone belts (20), or Archean sandstones and conglomerates (21). S-MIF only occurred in Earth's atmosphere before the Great Oxygenation Event at *ca.* 2.45 Ga (22), so its presence in at least part of the Pitcairn plume source places a strong lower limit on the age of that source. The association of nonchondritic $\delta^{34}S$ (between $-6.1‰$ and $-2.3‰$) with negative $\Delta^{33}S$ is an unambiguous signal of a contribution of Archean supracrustal material to the plume source.

Cabral et al. (23) reported small negative S-MIF anomalies for sulfides in HIMU basalts from Mangaia Island (Fig. 2), which they attributed to hydrothermal processes occurring in Archean basaltic crust. Interestingly, at both Pitcairn and Mangaia, $\Delta^{33}S$ are always negative, in contrast to values found in sublithospheric sulfide included in diamonds.

Previous modeling (3, 12, 13) suggested that the Pitcairn source includes recycled surface material, although with a young age (0.7 Ga to 2 Ga). To investigate the elemental and isotopic composition of the Pitcairn component, we developed a mixing model using our new Pb, Sr, Nd, and Hf data for Pitcairn (see *Materials and Methods* and *SI Appendix*, Table S2 and Fig. S2). This model constrains the isotopic ratios and Pb, Sr, Nd, and Hf concentrations of the Pitcairn component by assuming that it is the unknown member of a three-component mix (along with old subducted crust and ambient peridotitic mantle). The composition of the Pitcairn component (shown by the yellow star on Fig. 3 and *SI Appendix*, Fig. S3) is determined with no assumption about its geological origin but by simply adjusting its isotopic ratios and trace element concentrations so

that its calculated percentage in the source of each individual Pitcairn lava is the same for all available isotopic systems (Pb, Sr, Nd, and Hf).

Our mixing model provides two important pieces of information: (*i*) that the percentage of the Pitcairn component in the source of the individual lavas varies between ∼2.5% and ∼18% and (*ii*) that the Pitcairn component has a trace element composition (see *SI Appendix*, Table S3) that is significantly depleted relative to that modeled, for example, as a source component for the Gambier Island basalts (24), located upstream along the Pitcairn chain (also listed in *SI Appendix*, Table S3 and Fig. 1). The Gambier Island source was suggested to consist of 1.5-Ga recycled material (basaltic crust + average oceanic sediment) and ambient peridotite.

Using the modeled Pb isotopic composition of the Pitcairn component and the evidence for S-MIF at Pitcairn, we can use a three-stage Pb growth model including a Monte Carlo refinement procedure to constrain its age (T) and μ ($^{238}U/^{204}Pb$) and κ ($^{232}Th/^{238}U$) ratios. The Monte Carlo refinement technique (25) searches possible combinations of μ ($^{238}U/^{204}Pb$), κ ($^{232}Th/^{238}U$), and age for the three stages that reproduce the targeted Pitcairn component Pb isotopic values (see *Materials and Methods* and *SI Appendix*, Fig. S4). The method randomly tests potential growth-model results (for model equations, see *Materials and Methods*) with a criteria function (Eq. **4**) and either accepts or rejects the results depending on their match to the target value, here the yellow star in Fig. 3. The method is intrinsically not very different from the Monte Carlo simulation of Eisele et al. (13), but their target composition was different in two significant ways: (*i*) a $^{206}Pb/^{204}Pb$ lower than 17.6 when ours is 17.04, and (*ii*) variable $^{207}Pb/^{204}Pb$ and $^{208}Pb/^{204}Pb$ ($^{207}Pb/^{204}Pb$ ratio within ±0.005 from the array in $^{207}Pb/^{204}Pb$ vs. $^{206}Pb/^{204}Pb$ space and $^{208}Pb/^{204}Pb$ between 38.8 and 39.1) when ours are 15.45 and 39.0.

The three steps of our model are distinguished using subscripts 1, 2, and 3 for T, μ, and κ. T_1 corresponds to the age of the Earth (4.55 Ga), T_2 represents the onset of the crustal history, and T_3
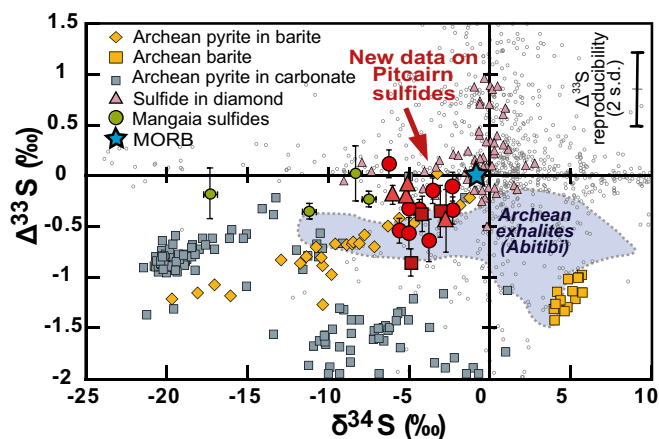
Fig. 2. $\Delta^{33}S$ versus $\delta^{34}S$ data for Pitcairn seamount sulfides, along with literature data. Red dots correspond to measurements on sulfides located in the matrix, red triangles correspond to sulfide inclusions within olivine, and red squares correspond to sulfide included in plagioclase. Also shown are data reported recently on sulfides hosted in olivine crystals from Mangaia Island (23), Archean barite and pyrite hosted in barite (16, 17), Archean pyrite hosted in carbonate (18, 19, 42), sulfide inclusions in diamonds (41), and exhalites from the Abitibi greenstone belt (blue field) (20). The gray dots correspond to previously published sulfur isotope data after figure 1 in ref. 43. Errors bars on each data point correspond to calculated propagated errors on $\Delta^{33}S$ and $\delta^{34}S$ (95% confidence, smaller than symbols for $\delta^{34}S$; see *SI Appendix* and *SI Appendix*, Table S1A). The external error on $\Delta^{33}S$ shown using a vertical bar at the top of the diagram was calculated using the repeatability on standards [$\Delta^{33}S = 0.37$ at 2 standard deviation (s.d.)]. The $\delta^{34}S$ is defined as $\delta^{34}S = 1,000 \times [(^{34}S/^{32}S_{sample})/(^{34}S/^{32}S_{CDT}) - 1]$ and $\Delta^{33}S$ as $\Delta^{33}S = \delta^{33}S - 1,000 \times \{[1 + (\delta^{34}S/1,000)]^{0.515} - 1\}$, with $\delta^{33}S = 1,000 \times [(^{33}S/^{32}S_{sample})/(^{33}S/^{32}S_{CDT}) - 1]$, and CDT is the Canyon Diablo Troilite standard.

represents the age of the onset of the surface material history. To limit the number of possible solutions, we set four values, the age of the Earth (T_1) and the initial composition of its mantle [$\mu_1 = 8.3$ and $\kappa_1 = 3.8$ (26)] together with the age (T_2) of the onset of crustal history [here 3 Ga (27, 28)] (see *Materials and Methods* for the choice of parameters). Results are shown in Fig. 4 in both $\mu_2-\kappa_2-\kappa_3$ and $\mu_2-\kappa_2-T_3$ space, and other interdependencies between μ_2, κ_2, μ_3, κ_3, and T_3 are shown in *SI Appendix*, Fig. S5. Fig. 4 shows that a large number of $\mu-\kappa-T$ combinations (all dots in Fig. 4) can reproduce the target composition but that, by limiting the range of μ_2 and κ_2 to values reasonable for the continental crust [$9 \leq \mu_2 \leq 11.6$ and $4 \leq \kappa_2 \leq 5$ (29–33); see Fig. 4A], the field is drastically reduced (as shown by the red dots). We can use the presence of S-MIF in the Pitcairn component to place a lower limit of 2.45 Ga on T_3 (the onset of sedimentary history); the μ_2 and κ_2 constraints outlined above give an upper age limit for T_3 of 2.75Ga, with a maximum of solutions around 2.5 Ga to 2.6 Ga. This Archean age for the Pitcairn component differs greatly from the 0.7- to 2-Ga model ages suggested previously (12, 13). This difference results from the combined effects of the different composition of the Pitcairn component, the older onset of crustal evolution (3.7 Ga), and, mainly, the lower μ and higher κ values for the early mantle (13) used in previous modeling.

Our model provides constraints on the μ and κ values of the sedimentary material formed at T_3 and recycled later on into the mantle. The calculated low values for μ_3 (6.3 to 6.4) and high values for κ_3 (6.3 to 6.7) are needed to produce the high $^{208}Pb/^{204}Pb$ at low $^{206}Pb/^{204}Pb$ that characterize EM I. We also tested the model for variations in the age of onset of crustal history (T_2) ranging from 2.5 Ga to 3.8 Ga to evaluate the impact of this parameter on the final results. The main findings are (*i*) when the age of the crustal history onset increases from 2.5 Ga to 3.8 Ga, κ_3 (the sedimentary component value) needs to decrease from 6.6 through 7.4

($T_2 = 2.5$ Ga) to 5.3 through 5.8 ($T_2 = 3.8$ Ga) but remains at high values (see *SI Appendix*, Fig. S6); (*ii*) in all cases, the age of onset of the sedimentary history (T_3) is Archean or very early Proterozoic (~2.3 Ga if $T_2 = 2.5$ Ga and ~3.5 Ga if $T_2 = 3.8$ Ga) (see *SI Appendix*, Fig. S6); and (*iii*) the overall probability of the model reproducing the lead isotopic values of the Pitcairn component decreases significantly when T_2 increases (with an increase of T_2 from 2.5 Ga to 3.8 Ga, the probability of successful results decreases from ~25% to ~2.5%; see *SI Appendix*, Fig. S6).

Together with its low μ and high κ (and ancient negative $\Delta^{33}S$), the Archean Pitcairn component has very low Pb, Nd, and Hf concentrations and rather low Sr contents (see *SI Appendix*, Fig. S5 and Table S3). Equivalent concentrations are not seen in modern oceanic
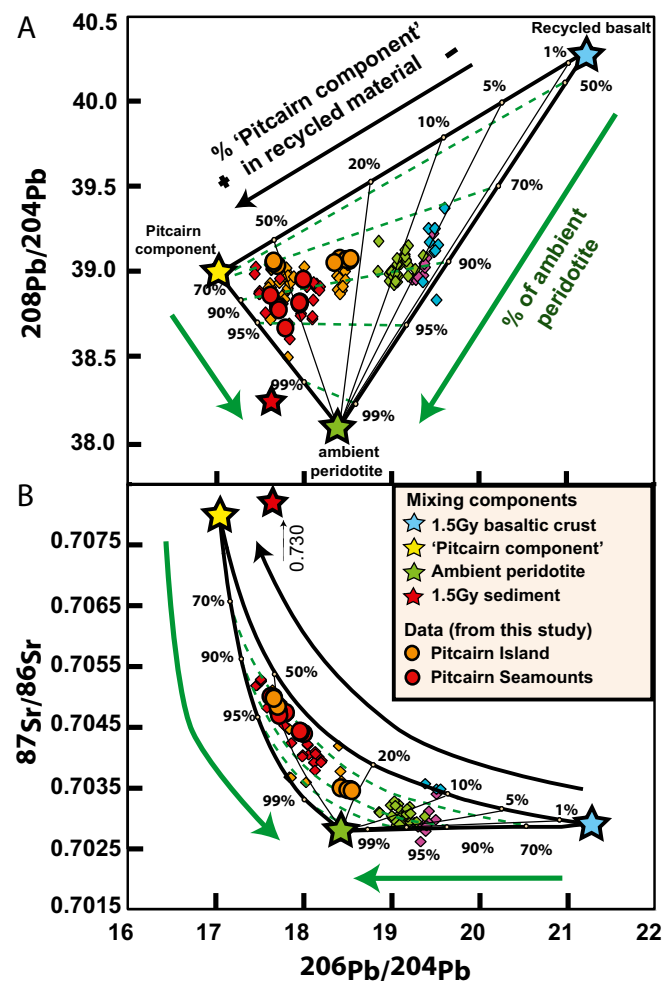

Fig. 3. Mixing arrays in (*A*) $^{208}Pb/^{204}Pb$ and (*B*) $^{87}Sr/^{86}Sr$ versus $^{206}Pb/^{204}Pb$ isotopic spaces. Orange and red circles show new data obtained on Pitcairn Island and Pitcairn Seamounts. Also shown are the compositions of the endmembers used in the mixing modeling of the Pitcairn data: 1.5-Ga basaltic crust (blue star) and ambient mantle peridotite (green star) as suggested previously for other islands along the Pitcairn chain (24) and the Pitcairn component (yellow star). The 1.5-Ga sediment suggested for the Gambier source is shown with a red star. The isotopic ratios and element concentrations of all endmembers are given in *SI Appendix*, Table S3. Thick black lines delimit the field in which all mixtures lie, green dashed lines show percentages of ambient peridotite in the source of magmas, and thin black lines connect ambient peridotite and different mixing proportions of Pitcairn component with recycled basaltic crust. Parameters for mixing models are given in *SI Appendix*, Table S3. Literature data are shown with diamonds: Mururoa (blue) (44–47), Fangataufa (purple) (45, 46, 48), Gambier (green) (24, 45, 46, 49), and Pitcairn Island and seamounts (orange and red) (8, 12, 13, 50, 51).
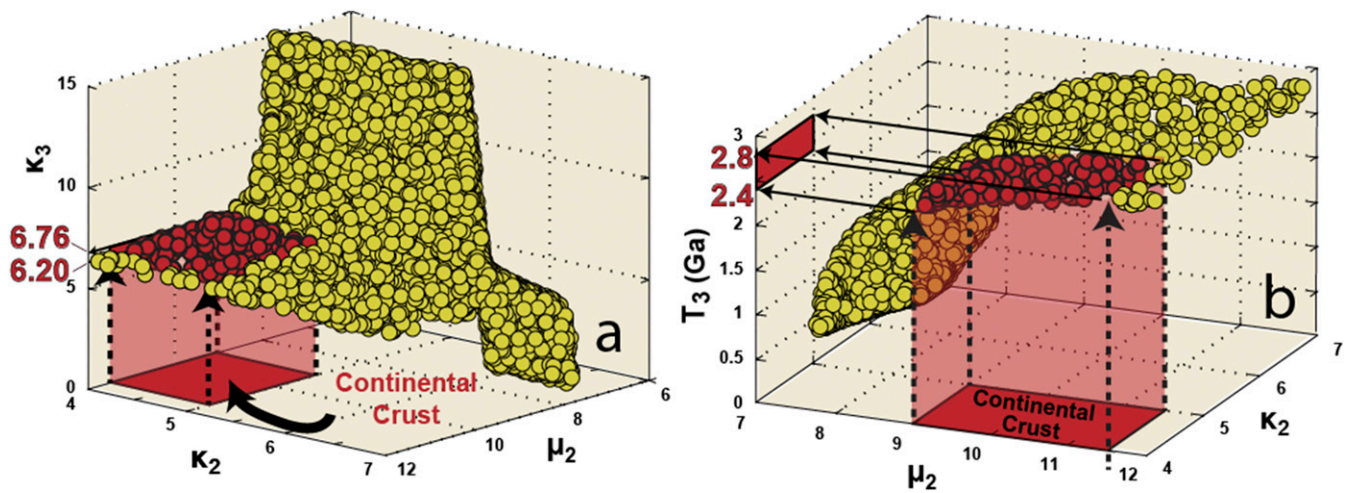
Fig. 4. Results of the Monte Carlo refinement modeling showing the interdependencies of parameters in the three-stage Pb evolution model. (*A*) The interdependence between κ_2, μ_2, and κ_3 and (*B*) the interdependence between μ_2, κ_2, and T_3. Only values fitting the target Pitcairn component ($^{206}Pb/^{204}Pb$ = 17.04, $^{207}Pb/^{204}Pb$ = 15.45, and $^{208}Pb/^{204}Pb$ = 39) are represented (see *Results and Discussion* and *Materials and Methods* for more details). Model limits are described in *Results and Discussion* and in *Materials and Methods*. The red fields show our preferred range of μ_2 (9 to 11.6) and κ_2 (4, 5) for continental crust, and the red dots highlight solutions with values in these ranges that also have T_3 ages > 2.45 Ga in accordance with the S-MIF evidence.

sediments (see *SI Appendix*, Table S4 for a comparison), suggesting they may be a feature unique to Archean surface materials.

However, few Archean materials known are so chemically depleted and also match the negative $\Delta^{33}S$ and $\delta^{34}S$. Archean continental paleosols, for example, have been reported (21) to show systematically negative $\Delta^{33}S$ values, but their trace element concentrations appear too high to fit the requirements of our model. Much more likely candidates, which also show negative $\Delta^{33}S$, are Neo-Archean carbonates, such as those found in South Africa and Brazil (18, 19) and exhalite sedimentary deposits, such as are found in the Abitibi greenstone belt (Fig. 2). The latter deposits consist of an alternation of cherts, silicate facies iron formation, and graphitic argillite (20). Such ultrasiliceous sediments are usually very depleted in most trace elements (34, 35) and were deposited in abundance during the earliest part of Earth history (36, 37). Although some of the trace element contents of Archean sediments do not fully match the values required by our model (see *SI Appendix*, Table S4), modification of their compositions by dehydration/melting processes during subduction (38) could have removed significant proportions of their trace elements without seriously affecting the $\Delta^{33}S$ signature (39). Subduction of such sediments, which ultimately are derived from the Archean continents, therefore appears the best explanation for the low μ, high κ, and negative S-MIF of the Pitcairn component.

Whereas photochemical reactions in the Archean atmosphere produced negative and positive mass-independent anomalies in the same proportion, one remarkable feature of the Archean surface S-MIF record preserved today is the overabundance of positive $\Delta^{33}S$ anomalies (19, 40). This finding suggests that negative $\Delta^{33}S$ are preserved in a reservoir that has not yet been found. Sulfide inclusions in diamond mainly preserve positive $\Delta^{33}S$ signatures (41), indicating that the missing reservoir is not the sublithospheric mantle. Cabral et al. (23), working on the HIMU island Mangaia, reported negative S-MIF in sulfide inclusions in olivine and attributed this to recycling of hydrothermally altered Archean oceanic crust; together with our evidence for negative S-MIF in a Pitcairn component that probably represents subducted, continent-derived sediments, this suggests that a large variety of Archean seafloor materials had negative S-MIF that are now stored in areas of the deep mantle sampled by plumes. The deep mantle might, therefore, be a promising candidate for the missing negative $\Delta^{33}S$ reservoir; if that is the case, this reservoir has survived in the deep mantle for billions of years without being completely mixed with the surrounding peridotite.

Materials and Methods

Radiogenic Isotopes. All samples were crushed in an agate mortar, and the pure Nd, Hf, Pb, and Sr fractions were isolated using ion exchange chromatography techniques. Nd, Hf, and Pb isotopic ratios were measured using a high-resolution multicollector inductively coupled plasma mass spectrometer (MC-ICP-MS; Nu Instrument 500 HR) at ENS Lyon, and Sr isotopic ratios using a thermal ionization mass spectrometer (TIMS, Thermo Scientific Triton) at PSO-IUEM (Pôle de Spectrométrie Océan, Institut Universitaire Européen de la Mer) in Brest (see *SI Appendix* for more details).

Sulfur Isotopes. Multiple sulfur isotope analyses ($\delta^{33}S$, $\delta^{34}S$, $\Delta^{33}S$) were performed in situ on thin sections using a high-resolution secondary ion mass spectrometer (CAMECA 1280-HR, CRPG-Nancy) (see *SI Appendix* for more details).

Monte Carlo Refinement Method. The three-stage Pb isotopic growth is described by Eqs. 1–3 for the three isotopic ratios $^{206}Pb/^{204}Pb$, $^{207}Pb/^{204}Pb$, and $^{208}Pb/^{204}Pb$,

$$\frac{^{206}Pb}{^{204}Pb} = \left(\frac{^{206}Pb}{^{204}Pb}\right)i + \mu_1\left(e^{\lambda a^* T_1} - e^{\lambda a^* T_2}\right) + \mu_2\left(e^{\lambda a^* T_2} - e^{\lambda a^* T_3}\right) + \mu_3\left(e^{\lambda a^* T_3} - 1\right), \quad [1]$$

$$\frac{^{207}Pb}{^{204}Pb} = \left(\frac{^{207}Pb}{^{204}Pb}\right)i + \frac{\mu_1}{137.8}\left(e^{\lambda b^* T_1} - e^{\lambda b^* T_2}\right) + \frac{\mu_2}{137.8}\left(e^{\lambda b^* T_2} - e^{\lambda b^* T_3}\right) + \frac{\mu_3}{137.8}\left(e^{\lambda b^* T_3} - 1\right), \quad [2]$$

$$\frac{^{208}Pb}{^{204}Pb} = \left(\frac{^{208}Pb}{^{204}Pb}\right)i + \omega_1\left(e^{\lambda c^* T_1} - e^{\lambda c^* T_2}\right) + \omega_2\left(e^{\lambda c^* T_2} - e^{\lambda c^* T_3}\right) + \omega_3\left(e^{\lambda c^* T_3} - 1\right), \quad [3]$$

where T_1 is the age of the Earth (4.55 Ga), and T_2 and T_3 represent the onset of the crustal (T_2) and sedimentary (T_3) histories; $(^{20*}Pb/^{204}Pb)_i$ is the isotopic ratio at Earth's formation, taken as that of Canyon Diablo Troilite; λ_a, λ_b, and λ_c are the decay constants of ^{238}U, ^{235}U, and ^{232}Th, respectively; $\mu = ^{238}U/^{204}Pb$, $\omega = ^{232}Th/^{204}Pb$; and $\kappa = \omega/\mu = ^{232}Th/^{238}U$.

To reproduce the Pb isotopic ratios of the Pitcairn component as listed in *SI Appendix*, Table S3, we performed a Monte Carlo refinement of the possible combinations of μ ($^{238}U/^{204}Pb$), κ ($^{232}Th/^{238}U$) and age that fulfill the three equations given above. The method consists in generating random values for each unknown parameter in Eq. 1–3. A comparison between calculated results for each random set of values and the problem statement (Pb isotopic composition of the Pitcairn component) allows the input parameters to be accepted or rejected. We performed a total of 1×10^{11} calculations. The results shown in Fig. 3 correspond to the 9,366 successful combinations. The only fixed parameters were age of the Earth at 4.55 Ga (T_1), initial mantle μ_1 and κ_1 at 8.3 and 3.8 (26) (the μ_1 corresponds to the average of values listed by Asmerom and Jacobsen (26) after removal the two outliers), and T_2 of 3 Ga for the time at which large volumes of continental crust already existed (27, 28). The unknown values are therefore μ_2, κ_2, μ_3, κ_3, and T_3. To investigate the variability of results, parameter

boundaries were set as follows: μ_2 was allowed to vary between 1 and 12, κ_2 was allowed to vary between 4 and 7, μ_3 was allowed to vary between 1 and 15, and κ_3 was allowed to vary between 1 and 15. Finally, the randomly generated sets of values were accepted as plausible only when the difference between the calculated Pb isotopic values and the target isotopic values of the Pitcairn component was less than 0.01 as shown in

$$\text{abs}\left(\left(\frac{^{206}\text{Pb}}{^{204}\text{Pb}}\right)_{\text{target}} - \left(\frac{^{206}\text{Pb}}{^{204}\text{Pb}}\right)_a\right) + \text{abs}\left(\left(\frac{^{207}\text{Pb}}{^{204}\text{Pb}}\right)_{\text{target}} - \text{eq}\left(\frac{^{207}\text{Pb}}{^{204}\text{Pb}}\right)_b\right) \quad [4]$$
$$+ \text{abs}\left(\left(\frac{^{208}\text{Pb}}{^{204}\text{Pb}}\right)_{\text{target}} - \left(\frac{^{208}\text{Pb}}{^{204}\text{Pb}}\right)_c\right) < 0.01,$$

where the subscript "target" represents the Pitcairn component value and the subscripts a, b, and c refer to the results of Eqs. 1–3, respectively,

defined above. The Matlab code used for this model is available as Dataset S1.

1. Zindler A, Hart S (1986) Chemical geodynamics. *Annu Rev Earth Planet Sci* 14(1): 493–571.
2. Hofmann AW (1997) Mantle geochemistry: The message from oceanic volcanism. *Nature* 385(6613):219–229.
3. Chauvel C, Hofmann AW, Vidal P (1992) HIMU-EM: The French Polynesian connection. *Earth Planet Sci Lett* 110(1-4):99–119.
4. Stracke A, Bizimis M, Salters VJM (2003) Recycling oceanic crust: Quantitative constraints. *Geochem Geophys Geosyst* 4(3):8003.
5. Workman RK, Eiler JM, Hart SR, Jackson MG (2008) Oxygen isotopes in Samoan lavas: Confirmation of continent recycling. *Geology* 36(7):551–554.
6. Hémond C, Devey CW, Chauvel C (1994) Source compositions and melting processes in the Society and Austral plumes (South Pacific Ocean): Element and isotope (Sr, Nd, Pb, Th) geochemistry. *Chem Geol* 115(1-2):7–45.
7. Lassiter JC, Blichert-Toft J, Hauri EH, Barsczus HG (2003) Isotope and trace element variations in lavas from Raivavae and Rapa, Cook–Austral islands: Constraints on the nature of HIMU- and EM-mantle and the origin of mid-plate volcanism in French Polynesia. *Chem Geol* 202(1-2):115–138.
8. Woodhead JD, Devey CW (1993) Geochemistry of the Pitcairn seamounts, I: Source character and temporal trends. *Earth Planet Sci Lett* 116(1-4):81–99.
9. Cordier C, Chauvel C, Hémond C (2016) High-precision lead isotopes and stripy plumes: Revisiting the Society chain in French Polynesia. *Geochim Cosmochim Acta* 189:236–250.
10. Duncan RA, McDougall I, Carter RM, Coombs DS (1974) Pitcairn Island—Another Pacific hot spot? *Nature* 251(5477):679–682.
11. Binard N, Hékinian R, Stoffers P (1992) Morphostructural study and type of volcanism of submarine volcanoes over the Pitcairn hot spot in the South Pacific. *Tectonophysics* 206(3-4):245–264.
12. Woodhead J, McCulloch TM (1989) Ancient seafloor signals in Pitcairn Island lavas and evidence for large amplitude, small length-scale mantle heterogeneities. *Earth Planet Sci Lett* 94(3-4):257–273.
13. Eisele J, et al. (2002) The role of sediment recycling in EM-1 inferred from Os, Pb, Hf, Nd, Sr isotope and trace element systematics of the Pitcairn hotspot. *Earth Planet Sci Lett* 196(3):197–212.
14. McKenzie D, O'Nions RK (1983) Mantle reservoirs and ocean island basalts. *Nature* 301(5897):229–231.
15. Willbold M, Stracke A (2010) Formation of enriched mantle components by recycling of upper and lower continental crust. *Chem Geol* 276(3-4):188–197.
16. Shen Y, Farquhar J, Masterson A, Kaufman AJ, Buick R (2009) Evaluating the role of microbial sulfate reduction in the early Archean using quadruple isotope systematics. *Earth Planet Sci Lett* 279(3-4):383–391.
17. Ueno Y, Ono S, Rumble D, Maruyama S (2008) Quadruple sulfur isotope analysis of ca. 3.5 Ga Dresser Formation: New evidence for microbial sulfate reduction in the early Archean. *Geochim Cosmochim Acta* 72(23):5675–5691.
18. Zhelezinskaia I, Kaufman AJ, Farquhar J, Cliff J (2014) Large sulfur isotope fractionations associated with Neoarchean microbial sulfate reduction. *Science* 346(6210): 742–744.
19. Farquhar J, Zerkle AL, Bekker A (2014) Geologic and geochemical constraints on Earth's early atmosphere. *Treatise on Geochemistry* (Elsevier, Oxford), 2nd Ed, pp 91–129.
20. Hiebert RS, Bekker A, Houlé MG, Rouxel OJ, Wing BA (2015) Identifying and tracing crustal contamination in the Hart komatiite-associated Ni-Cu-(PGE) deposit using multiple S and Fe isotopes: Abitibi greenstone belt, Ontario. *Targeted Geoscience Initiative 4: Canadian Nickel-Copper-Platinum Group Elements-Chromium Ore Systems–Fertility, Pathfinders, New and Revised Models*, Open File Report, eds Ames DE, Houlé MG, (Geol Surv Canada, Ottawa), Vol 7856, pp 197–207, 305 pp.
21. Maynard JB, Sutton SJ, Rumble Iii D, Bekker A (2013) Mass-independently fractionated sulfur in Archean paleosols: A large reservoir of negative Δ33S anomaly on the early Earth. *Chem Geol* 362:74–81.
22. Farquhar J, Bao H, Thiemens M (2000) Atmospheric influence of Earth's earliest sulfur cycle. *Science* 289(5480):756–759.
23. Cabral RA, et al. (2013) Anomalous sulphur isotopes in plume lavas reveal deep mantle storage of Archaean crust. *Nature* 496(7446):490–493.
24. Delavault H, Chauvel C, Sobolev A, Batanova V (2015) Combined petrological, geochemical and isotopic modeling of a plume source: Example of Gambier Island, Pitcairn chain. *Earth Planet Sci Lett* 426:23–35.
25. Anderssen RS (1972) A refinement procedure for pure random search. *Inf Process Lett* 1(5):197–200.
26. Asmerom Y, Jacobsen SB (1993) The Pb isotopic evolution of the Earth: Inferences from river water suspended loads. *Earth Planet Sci Lett* 115(1-4):245–256.
27. Dhuime B, Hawkesworth CJ, Cawood PA, Storey CD (2012) A change in the geodynamics of continental growth 3 billion years ago. *Science* 335(6074):1334–1336.
28. Pujol M, Marty B, Burgess R, Turner G, Philippot P (2013) Argon isotopic composition of Archaean atmosphere probes early Earth geodynamics. *Nature* 498(7452):87–90.
29. Allègre CJ, Lewin E (1989) Chemical history of the Earth: Evidence from global non-linear inversion of isotopic data in a three box model. *Earth Planet Sci Lett* 96(1-2):61–88.
30. Garçon M, Chauvel C, France-Lanord C, Limonta M, Garzanti E (2013) Removing the "heavy mineral effect" to obtain a new Pb isotopic value for the upper crust. *Geochem Geophys Geosyst* 14(9):3324–3333.
31. Kramers JD (2002) Global modelling of continent formation and destruction through geological time and implications for CO2 drawdown in the Archaean Eon. *Geol Soc Lond Spec Publ* 199(1):259–274.
32. Stacey JS, Kramers JD (1975) Approximation of terrestrial lead isotope evolution by a two-stage model. *Earth Planet Sci Lett* 26(2):207–221.
33. Zartman RE, Haines SM (1988) The plumbotectonic model for Pb isotopic systematics among major terrestrial reservoirs—A case for bi-directional transport. *Geochim Cosmochim Acta* 52(6):1327–1339.
34. Spier CA, de Oliveira SMB, Sial AN, Rios FJ (2007) Geochemistry and genesis of the banded iron formations of the Cauê Formation, Quadrilátero Ferrífero, Minas Gerais, Brazil. *Precambrian Res* 152(3-4):170–206.
35. Sugitani K (1992) Geochemical characteristics of Archean cherts and other sedimentary rocks in the Pilbara Block, Western Australia: Evidence for Archean seawater enriched in hydrothermally-derived iron and silica. *Precambrian Res* 57(1-2):21–47.
36. Eriksson PG, et al. (1998) Precambrian clastic sedimentation systems. *Sediment Geol* 120(1-4):5–53.
37. Lowe DR (1999) Petrology and sedimentology of cherts and related silicified sedimentary rocks in the Swaziland Supergroup. *Spec Pap Geol Soc Am* 329:83–114.
38. McCulloch MT, Gamble JA (1991) Geochemical and geodynamical constraints on subduction zone magmatism. *Earth Planet Sci Lett* 102(3-4):358–374.
39. Evans KA, Powell R (2015) The effect of subduction on the sulphur, carbon and redox budget of lithospheric mantle. *J Metamorph Geol* 33(6):649–670.
40. Farquhar J, Wing BA (2003) Multiple sulfur isotopes and the evolution of the atmosphere. *Earth Planet Sci Lett* 213(1-2):1–13.
41. Thomassot E, et al. (2009) Metasomatic diamond growth: A multi-isotope study (^{13}C, ^{15}N, ^{33}S, ^{34}S) of sulphide inclusions and their host diamonds from Jwaneng (Botswana). *Earth Planet Sci Lett* 282(1-4):79–90.
42. Farquhar J, et al. (2013) Pathways for Neoarchean pyrite formation constrained by mass-independent sulfur isotopes. *Proc Natl Acad Sci USA* 110(44):17638–17643.
43. Johnston DT (2011) Multiple sulfur isotopes and the evolution of Earth's surface sulfur cycle. *Earth Sci Rev* 106(1-2):161–183.
44. Caroff M, Maury R, Guille G, Bellon H, Cotten J (1993) Les basaltes de l'Archipel des Gambier (Polynésie française) [Basalts from the Gambier Archipelago (French Polynesia)]. *C R Acad Sci Paris* 317(3):359–366.
45. Dostal J, Cousens B, Dupuy C (1998) The incompatible element characteristics of an ancient subducted sedimentary component in ocean island basalts from French Polynesia. *J Petrol* 39(5):937–952.
46. Dupuy C, Vidal P, Maury R, Guille G (1993) Basalts from Mururoa, Fangataufa and Gambier islands (French Polynesia): Geochemical dependence on the age of the lithosphere. *Earth Planet Sci Lett* 117(1-2):89–100.
47. Maury R, et al. (1992) Mururoa Atoll French Polynesia; II, Magmatic sequence. *Bull Soc Geol Fr* 8(5):659–679.
48. Bardintzeff J-M, Demange J, Gachon A (1986) Petrology of the volcanic bedrock of Mururoa atoll (Tuamotu Archipelago, French Polynesia). *J Volcanol Geotherm Res* 28(1-2):55–83.
49. Cotten J, et al. (1995) Origin of anomalous rare-earth element and yttrium enrichments in subaerially exposed basalts: Evidence from French Polynesia. *Chem Geol* 119(1):115–138.
50. Eiler JM, et al. (1995) Oxygen isotope evidence against bulk recycled sediment in the mantle sources of Pitcairn Island lavas. *Nature* 377(6545):138–141.
51. Honda M, Woodhead J (2005) A primordial solar-neon enriched component in the source of EM-I-type ocean island basalts from the Pitcairn Seamounts, Polynesia. *Earth Planet Sci Lett* 236(3-4):597–612.

Delavault et al.